

# The Wigner flow on the sphere

Popo Yang<sup>1</sup>, Iván F Valtierra<sup>2</sup>, Andrei B Klimov<sup>2</sup>, Shin-Tza Wu<sup>3</sup>,  
Ray-Kuang Lee<sup>1</sup>, Luis L Sánchez-Soto<sup>4,5</sup> and Gerd Leuchs<sup>5,6,7</sup>

**Abstract.** We derive a continuity equation for the evolution of the SU(2) Wigner function under nonlinear Kerr evolution. We give explicit expressions for the resulting quantum Wigner current, and discuss the appearance of the classical limit. We show that the global structure of the quantum current significantly differs from the classical one, which is clearly reflected in the form of the corresponding stagnation lines.

<sup>1</sup>Department of Physics, National Tsing Hua University, Hsinchu 300, Taiwan

<sup>2</sup>Departamento de Física, Universidad de Guadalajara, 44420 Guadalajara, Jalisco, Mexico

<sup>3</sup>Department of Physics, National Chung Cheng University, Chiayi 621, Taiwan

<sup>4</sup>Departamento de Óptica, Facultad de Física, Universidad Complutense, 28040 Madrid, Spain

<sup>5</sup>Max-Planck-Institut für die Physik des Lichts, Staudtstraße 2, 91058 Erlangen, Germany

<sup>6</sup>Department of Physics, University of Erlangen-Nuremberg, Staudtstraße 7 B2, 91058 Erlangen, Germany

<sup>7</sup>Physics Department, Centre for Research in Photonics, University of Ottawa, Advanced Research Complex, 25 Templeton, Ottawa ON Canada, K1N 6N5

## 1. Introduction

In classical statistical mechanics, an ensemble of particles is described by a distribution function  $f(x, p|t)$  that depends on the phase-space variables  $x$  and  $p$  and evolves in time. The corresponding dynamics is governed by the Liouville equation [1], which asserts that for conservative forces  $f(x, p|t)$  is constant along the trajectories of the system. In other words, the local density of points traveling through phase-space is constant with time. This conservation can be succinctly summarized as a continuity equation

$$\frac{\partial f(x, p|t)}{\partial t} = -\nabla \cdot \mathbf{J}(x, p|t), \quad (1.1)$$

where  $\mathbf{J}(x, p|t)$  is a probability current. Indeed, this flow is regular [2] and largely determined by location and nature of its stagnation points; i.e, those points for which  $\mathbf{J} = 0$ . For conservative systems, the form of  $J(x, p|t)$  immediately follows from the corresponding Poisson brackets.

This scenario can be extended to more general systems admitting a dynamical symmetry group. This enables the construction of a phase space  $\mathcal{M}$  as an appropriate homogeneous manifold [3, 4]. This classical formulation associates a probability with every point  $\Omega \in \mathcal{M}$ . However, in the quantum domain the uncertainty principle does not allow one to attribute a state to a single point in phase space [5–9]. Because of this fundamental difference, there is no unique way of defining a quantum probability distribution. The Wigner function  $W_\rho(\Omega)$  is perhaps the closest to the analogous counterpart. Note that, although the Wigner function has the correct marginal probability distributions, it can itself be negative.

In the phase-space approach, every observable  $\hat{A}$  is mapped onto a function  $W_A(\Omega)$  (called its Weyl symbol). In particular, the Weyl symbol of the density matrix is precisely the Wigner function and its time evolution reads

$$\partial_t W_\rho(\Omega|t) = \{W_\rho(\Omega), W_H(\Omega)\}_M, \quad (1.2)$$

where  $W_H(\Omega)$  is the symbol of the Hamiltonian and the Moyal bracket  $\{\cdot, \cdot\}_M$  is the image of the quantum commutator [times  $(i\hbar)^{-1}$ ] under the Weyl map [10]. The resulting partial differential equation contains, in general, higher-order derivatives, which significantly complicate the search for an exact solution. However, it admits a natural expansion in powers of a semiclassical parameter  $\varepsilon \ll 1$  that characterizes the strength of quantum fluctuations in the system. This parameter depends on the dynamical symmetry and, roughly speaking, is the inverse of the number of excitations [11]. To the lowest order in  $\varepsilon$ , equation (1.2) is of the Liouvillian form

$$\partial_t W_\rho(\Omega) = \varepsilon \{W_\rho(\Omega), W_H(\Omega)\} + O(\varepsilon^3), \quad (1.3)$$

where now  $\{\cdot, \cdot\}$  is the Poisson bracket in the manifold  $\mathcal{M}$ . The semiclassical or truncated Wigner approximation (TWA) [12–15] consists in disregarding the higher order terms, so that  $W_\rho(\Omega|t) \simeq W_\rho(\Omega(-t)|0)$ , where  $\Omega(t)$  are classical trajectories generated by  $W_H(\Omega)$ .

It has been pointed out [16–18], that one can construct a Wigner current  $\ddagger$  in such a way that the evolution can be mapped as a continuity equation very much analogous to (1.1). Surprisingly, this Wigner current, which is the equivalent of the classical Liouville flow, has, so far, not been studied in great detail [20–23]. The form of the current, and especially the behavior in the vicinity of its stagnation points, can be used for the characterization of the quantumness of the evolution (see also references [24–26], where the stagnation points of the Husimi  $Q$  function were studied).

In this paper, we extend these ideas to spinlike systems, where the classical phase space is the unit sphere. We stress that this is not a mere academic curiosity, since the underlying  $SU(2)$  symmetry plays a pivotal role in numerous models in physics [27].

In the spirit of equations (1.2) and (1.3), we introduce in a natural way the classical and quantum Wigner currents. We will show, using the simplest example of nonlinear Kerr dynamics, that the global structure of the quantum Wigner current significantly differs from the classical one. Such a difference is clearly observable even during the short-time evolution of semiclassical states (specified by localized distributions in phase space), when the Wigner distribution can still be well described in terms of the semiclassical approximation. In other words, the Wigner current allows us to distinguish between quantum and semiclassical dynamics, while the distributions evolved according to the Moyal and Poisson brackets are still quite similar. The stagnation points/lines of the classical Wigner current are basically determined by the zeros of the semiclassically evolved Wigner distribution. Therefore, the structure of the stagnation lines can be used for the analysis of the quantumness of the phase-space dynamics in the semiclassical limit. Furthermore, an extra benefit of bringing the Wigner current into play is that it can give a compelling visual representation of how nonclassical features arise during the evolution.

## 2. Wigner function on the sphere

We consider a system whose dynamical symmetry group is  $SU(2)$ . As heralded in the Introduction, we follow the ideas in references [3,4] to work out quasiprobability distributions

$\ddagger$  We will mainly call the quantity  $\mathbf{J}$  the Wigner current. However, it can also be interpreted as quasiprobability flow. For this reason, the designation Wigner flow has been used in the literature before. Note though that, as discussed in [19], no flow (in the sense of mapping of a distribution along trajectories) exists in the quantum domain.

on the sphere satisfying all the pertinent requirements. This construction was generalized by others [28–32] and has proved to be very useful in visualizing properties of spinlike systems [33–36].

The corresponding Lie algebra  $\mathfrak{su}(2)$  is spanned by the operators  $\{\hat{S}_x, \hat{S}_y, \hat{S}_z\}$  satisfying the angular momentum commutation relations

$$[\hat{S}_x, \hat{S}_y] = i\hat{S}_z, \quad (2.1)$$

and cyclic permutations (in units  $\hbar = 1$ , which will be used throughout). The Casimir operator is  $\hat{\mathbf{S}}^2 = \hat{S}_x^2 + \hat{S}_y^2 + \hat{S}_z^2 = S(S+1)\mathbb{1}$ , so the eigenvalue  $S$  (which is a nonnegative integer or half integer) labels the irreducible representations (irreps). We take a fixed irrep of spin  $S$ , with a  $2S+1$ -dimensional carrier space  $\mathcal{H}_S$  spanned by the standard angular momentum basis  $\{|Sm\rangle, m = -S, \dots, S\}$ , whose elements are simultaneous eigenstates of  $\hat{\mathbf{S}}^2$  and  $\hat{S}_z$ :

$$\hat{\mathbf{S}}^2|S, m\rangle = S(S+1)|S, m\rangle, \quad \hat{S}_z|S, m\rangle = m|S, m\rangle. \quad (2.2)$$

The highest weight state is  $|S, S\rangle$  and it is annihilated by the ladder operator  $\hat{S}_+$  (with  $\hat{S}_\pm = \hat{S}_x \pm i\hat{S}_y$ ). The isotropy subgroup (i.e., the largest subgroup that leaves the highest weight state invariant) consists of all the elements of the form  $\exp(i\chi\hat{S}_z)$ , so it is isomorphic to  $U(1)$ . The coset space is then  $SU(2)/U(1)$ , which is just the unit sphere  $\mathcal{S}_2$  and it is the classical phase space, the natural arena to describe the dynamics.

The  $SU(2)$  coherent states  $|\Omega\rangle$  (with  $\Omega = (\theta, \phi) \in \mathcal{S}_2$ ) are defined, up to a global phase, by the action of the displacement operator [37]

$$\hat{D}(\Omega) = \exp\left[\frac{1}{2}\theta(\hat{S}_+e^{-i\phi} - \hat{S}_-e^{i\phi})\right] \quad (2.3)$$

on the highest weight state, with explicit expression in terms of  $\Omega$  given by

$$\begin{aligned} |\Omega\rangle &= \hat{D}(\Omega)|S, S\rangle \\ &= \sum_{m=-S}^S \sqrt{\frac{(2S)!}{(S-m)!(S+m)!}} [\cos(\theta/2)]^{S+m} [\sin(\theta/2)]^{S-m} e^{-im\phi} |S, m\rangle. \end{aligned} \quad (2.4)$$

Operators acting in a  $\mathcal{H}_S$  can be mapped onto functions on  $\mathcal{S}_2$  by means of the Stratonovich-Weyl kernel. It can be concisely defined as [38]

$$\hat{w}(\Omega) = \sqrt{\frac{4\pi}{2S+1}} \sum_{K=0}^{2S} \sum_{q=-K}^K Y_{Kq}^*(\Omega) \hat{T}_{Kq}^S, \quad (2.5)$$

where  $Y_{Kq}(\Omega)$  are the spherical harmonics,  $*$  indicates complex conjugation, and  $\hat{T}_{Kq}^S$  are the irreducible tensor operators [39, 40]

$$\hat{T}_{Kq}^S = \sqrt{\frac{2K+1}{2S+1}} \sum_{m, m'=-S}^S C_{Sm, Kq}^{Sm'} |S, m'\rangle \langle S, m|, \quad (2.6)$$

$C_{Sm, Kq}^{Sm'}$  being the corresponding Clebsch-Gordan coefficient [41]. The symbol  $W_A$  of an operator  $\hat{A}$  is then defined as

$$W_A(\Omega) = \text{Tr}[\hat{A} \hat{w}(\Omega)]. \quad (2.7)$$

Since the tensors  $\hat{T}_{Kq}^S$  constitute an orthonormal basis for the operators acting on  $\mathcal{H}_S$ , any observable  $\hat{A}$  can be expanded as

$$\hat{A} = \sum_{K=0}^{2S} \sum_{q=-K}^K A_{Kq} \hat{T}_{Kq}^S, \quad (2.8)$$

with  $A_{Kq} = \text{Tr}[\hat{A}\hat{T}_{Kq}^{S\dagger}]$ ,  $\dagger$  standing for Hermitian conjugation. Therefore, the symbol of  $\hat{A}$  can be expressed as the sum of symbols of the tensor components

$$W_A(\Omega) = \sqrt{\frac{4\pi}{2S+1}} \sum_{K=0}^{2S} \sum_{q=-K}^K A_{Kq} Y_{Kq}^*(\Omega). \quad (2.9)$$

As some relevant examples we shall need in what follows we quote

$$\begin{aligned} \hat{S}_i &\mapsto W_{S_i}(\Omega) = \sqrt{S(S+1)} n_i, \\ \{\hat{S}_i, \hat{S}_j\} &\mapsto W_{\{S_i, S_j\}}(\Omega) = C_S n_i n_j, \\ \hat{S}_i^2 &\mapsto W_{S_i^2}(\Omega) = \frac{1}{2} C_S (n_i^2 - \frac{1}{3}) + \frac{1}{3} S(S+1), \end{aligned} \quad (2.10)$$

where the Latin indexes run the values  $\{i, j\} \in x, y, z$ ,  $\mathbf{n} = (\sin \theta \cos \phi, \sin \theta \sin \phi, \cos \theta)^t$  is a unit vector in the direction of spherical angles  $(\theta, \phi) \in \mathcal{S}_2$ , and  $C_S = [S(S+1)(2S-1)(2S+3)]^{1/2}$ .

The Wigner function is the symbol of the density operator  $\hat{\rho}$ . It is  $SU(2)$  covariant: under the action of a  $2S+1$ -dimensional irrep of  $SU(2)$  given by the matrix  $\hat{R}(\Omega)$  [that is,  $\hat{\rho}' = \hat{R}(\Omega') \hat{\rho} \hat{R}^{-1}(\Omega')$ ],  $W_\rho(\Omega)$  experiences the transformation

$$W_{\rho'}(\Omega) = W_\rho(R^{-1}\Omega), \quad (2.11)$$

so that it follows rotations rigidly without changing its form. In addition, we have the overlap relation

$$\text{Tr}(\hat{\rho}\hat{A}) = \frac{2S+1}{4\pi} \int_{\mathcal{S}_2} d\Omega W_\rho(\Omega) W_A(\Omega), \quad (2.12)$$

where  $d\Omega = \sin \theta d\theta d\phi$  is the invariant measure in  $\mathcal{S}_2$ .

For a coherent state  $|\Omega_0\rangle$ , the Wigner function can be computed directly from the definition (2.7) by taking into account that

$$\langle \Omega_0 | \hat{T}_{Kq}^S | \Omega_0 \rangle = (2S)! \sqrt{\frac{4\pi}{(2S-K)!(2S+K+1)!}} Y_{Kq}(\Omega_0). \quad (2.13)$$

The final results thus reads

$$W_{\Omega_0}(\Omega) = (2S)! \sum_{K=0}^{2S} \sqrt{\frac{2S+1}{(2S-K)!(2S+K+1)!}} P_K(\cos \zeta), \quad (2.14)$$

where  $\cos \zeta = \cos \theta \cos \theta_0 + \sin \theta \sin \theta_0 \cos(\phi - \phi_0)$  and  $P_K(w)$  are the Legendre polynomials.

To conclude, we stress that this approach assume a fixed  $S$ . In some instances, as in polarization optics, a superposition of different  $S$  arise [42, 43]. The formalism can be generalized to cover this more general situation [44].

### 3. Dynamics and Wigner current on the sphere

The exact evolution equation for the Wigner function  $W_\rho(\Omega)$  has been obtained in [13]. For arbitrary Hamiltonians [living in a  $(2S+1)$ -dimensional representation of the universal enveloping algebra of  $\mathfrak{su}(2)$ ] the expressions are quite involved. For simplicity, in what follows, we restrict ourselves to two simple examples of great interest in applications.

### 3.1. Linear Hamiltonians

First of all, we consider the dynamics generated by linear Hamiltonians

$$\hat{H}_L = \sum_i a_i \hat{S}_i \quad (3.1)$$

whose symbol can be directly inferred from (2.10). The exact phase-space evolution is given by the first-order partial differential equation

$$\partial_t W_\rho(\Omega|t) = \sum_i a_i \{W_\rho(\Omega|t), n_i\}, \quad (3.2)$$

where

$$\{f, g\} = \frac{1}{\sin \theta} (\partial_\phi f \partial_\theta g - \partial_\theta f \partial_\phi g) \quad (3.3)$$

is the Poisson bracket on the sphere  $\mathcal{S}_2$ . The evolution for the Wigner function is

$$W_\rho(\Omega|t) = W_\rho(\Omega(-t)|0), \quad (3.4)$$

where  $\Omega(t)$  denotes classical trajectories, which are solutions of the classical Hamiltonian equations. It thus corresponds to a rotation of the initial distribution.

Next, we observe that if the evolution can be recast in the form  $\partial_t W_\rho(\Omega|t) = \{A, B\}$ , it can be interpreted as a continuity equation with current given by

$$J_\theta = -A \partial_\theta B, \quad J_\phi = \frac{1}{\sin \theta} A \partial_\phi B. \quad (3.5)$$

Accordingly, the linear dynamics is generated by

$$J_\theta = \frac{1}{\sin \theta} W_\rho(\Omega|t) \sum_i a_i \partial_\phi n_i, \quad (3.6)$$

$$J_\phi = -W_\rho(\Omega|t) \sum_i a_i \partial_\theta n_i.$$

Since for these linear Hamiltonians the exact evolution is the classical Liouville equation [45], the quantum and classical currents are just the same.

For the particular case of  $\hat{H}_L = \omega \hat{S}_z$  the resulting components of Wigner current are:

$$J_\theta = 0, \quad (3.7)$$

$$J_\phi = \omega \sin \theta W_\rho(\theta, \phi - \omega t|0).$$

In the supplemental material, we present an animation of this current for an initial coherent state.

### 3.2. Kerr dynamics

For quadratic Hamiltonians, we content ourselves with the simplest case of the so-called Kerr medium [46, 47], which is described by

$$\hat{H} = \chi \hat{S}_z^2. \quad (3.8)$$

The ensuing dynamics has been examined in terms of the standard position-momentum phase space [48, 49] and the associated Wigner current has been recently discussed [50]. For the SU(2) Wigner function the evolution equation turns out to be [13, 31]

$$\partial_t W_\rho(\Omega|t) = -\frac{\chi}{\varepsilon} \cos \theta \hat{\Gamma}(\theta, \mathcal{L}^2) \partial_\phi W_\rho(\Omega|t), \quad (3.9)$$

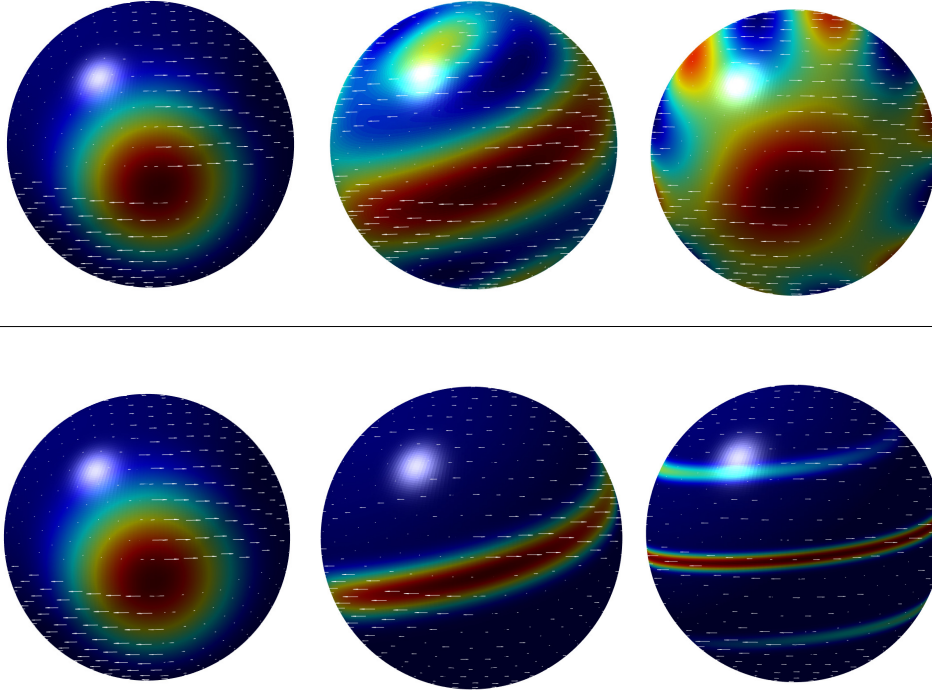


**Figure 1.** Snapshots of Kerr dynamics for an initial atomic coherent state ( $S = 10$ ) located in the equator at the dimensionless times  $\tau = 0$ ,  $\tau = 0.32$  and  $\tau = 1.5$ . Upper panel, quantum dynamics; lower panel, semiclassical evolution.

where  $\varepsilon = 1/(2S + 1)$  and the operator  $\hat{\Gamma}(\theta, \mathcal{L}^2)$  is

$$\hat{\Gamma}(\theta, \mathcal{L}^2) = \frac{1}{2}\Phi(\mathcal{L}^2) - \frac{\varepsilon^2}{2}(1 + 2 \tan \theta \partial_\theta)\Phi^{-1}(\mathcal{L}^2). \quad (3.10)$$

Here,  $\Phi(\mathcal{L}^2)$  is

$$\Phi(\mathcal{L}^2) = \left[ 2 - \varepsilon^2(2\mathcal{L}^2 + 1) + 2\sqrt{1 - \varepsilon^2(2\mathcal{L}^2 + 1) + \varepsilon^4\mathcal{L}^4} \right]^{1/2}, \quad (3.11)$$

and  $\Phi^{-1}(\mathcal{L}^2)$  its inverse. Both are functions solely of  $\mathcal{L}^2$ , which is a differential realization of the Casimir operator on  $\mathcal{S}_2$

$$\mathcal{L}^2 = - \left( \partial_{\theta\theta} + \cot \theta \partial_\theta + \frac{1}{\sin^2 \theta} \partial_{\phi\phi} \right), \quad (3.12)$$

and, consequently, we have  $\mathcal{L}^2 Y_{Kq}(\Omega) = K(K + 1)Y_{Kq}(\Omega)$ . Note also that the term between parentheses in (3.12) is the Laplace-Beltrami operator in  $\mathcal{S}_2$ .

Equation (3.9) can be represented in terms of the Poisson brackets as follows

$$\partial_t W_\rho(\Omega|t) = 2\varepsilon\chi \left\{ \hat{\Gamma}(\theta, \mathcal{L}^2) W_\rho(\Omega), \frac{1}{4\varepsilon^2} \cos^2 \theta \right\}. \quad (3.13)$$

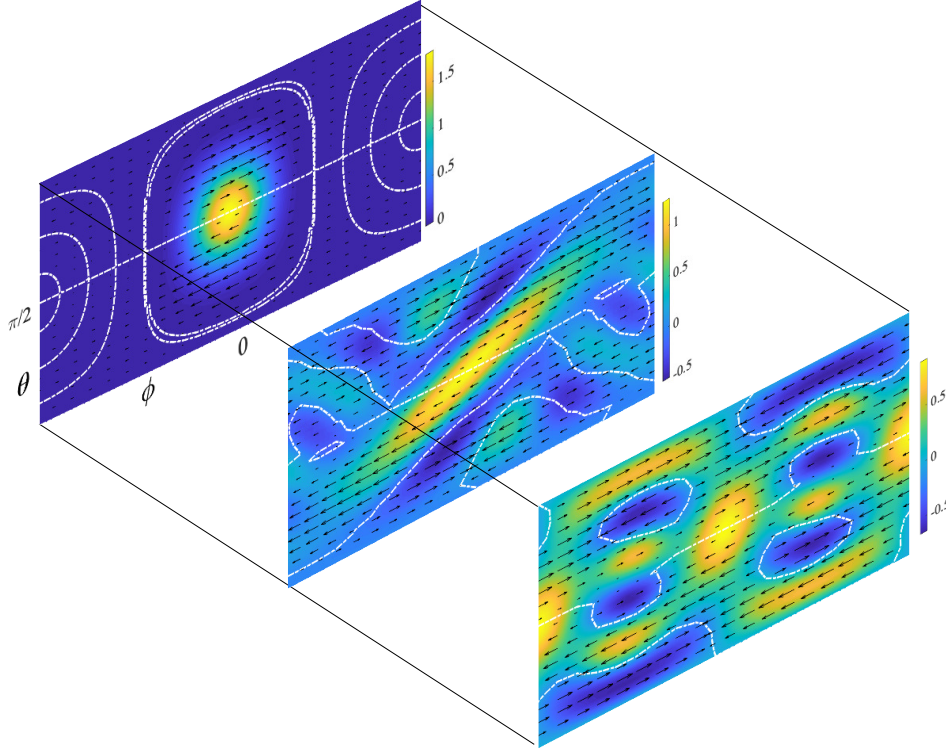


**Figure 2.** The quantum current in figure 1, but plotted in the plane (black arrows) for the same three times. The stagnation lines (white curves) separate regions of positive and negative values of the Wigner function.

Actually, the operator  $\hat{\Gamma}(\theta, \mathcal{L}^2)$  is responsible for the quantum deformation of the distribution. The current can be immediately found from (3.5):

$$J_\phi(t) = \chi \varepsilon^{-1} \sin \theta \cos \theta \hat{\Gamma}(\theta, \mathcal{L}^2) W_\rho(\Omega|t) \quad (3.14)$$

$$J_\theta(t) = 0.$$

The nonzero components of the current can be recast as

$$J_\phi(t) = \sin \theta \hat{U}(t) \frac{1}{\sin \theta} J_\phi(t=0), \quad (3.15)$$

where

$$\hat{U}(t) = \exp \left[ -\frac{\chi t}{\varepsilon} \cos \theta \hat{\Gamma}(\theta, \mathcal{L}^2) \partial_\phi \right] \quad (3.16)$$

is the evolution operator in phase space; that is,  $W_\rho(\Omega|t) = \hat{U}(t)W_\rho(\Omega|t=0)$ .

In figure 1 we plot the quantum current for an initial coherent state on the equator ( $\theta = \pi/2, \phi = 0$ ). We have chosen three different dimensionless times  $\tau = \chi t$  corresponding to  $\tau = 0$ ,  $\tau = 0.32$  (close to the best squeezing time) and  $\tau = 1.5$  (close to the appearance of two-component Schrödinger cats) for the case  $S = 10$ . The white arrows represent the current  $J_\phi$ . At  $\tau = 0$ , the size and position of the arrows clearly indicate the direction

of the deformation of the Wigner function: in the vicinity of the initial maximum, the *laminar flow* with increasing speed towards polar regions leads to the squeezing of the distribution along transverse directions for short times  $\tau \sim S^{-1/2}$ . Such a deformation is actually reflected in a real squeezing of  $\hat{S}_x$  and  $\hat{S}_y$  components. In addition, first signs of the quantum interference are observed. For cat times,  $\tau \sim 1$ , the structure of the quantum current is quite complicated: multiple regions where the current changes direction can be easily noticed. In the supplemental material, the reader can find an animation of this current for an initial coherent state.

To better appreciate the stagnation lines (recall that  $J_\theta = 0$  identically), in figure 2 we plot the Wigner current of figure 1, but now in the plane. There is always a trivial zero line at  $\theta = \pi/2$ . At the initial moment, the stagnation lines separate regions of positive and negative values of the Wigner function, as well as the minima of the negative ripples. New zero lines around negative parts of the Wigner distribution appear at the best squeezing time. Finally, nontrivial stagnation lines take the form of closed curves rounding minima of the interference pattern. These stagnation lines thus provide a complementary picture of quantum interference in phase space.

### 3.3. Semiclassical limit

The semiclassical limit in spinlike systems is related to large value of spin, naturally characterized by the parameter  $\varepsilon \ll 1$ . The semiclassical states are usually associated with smooth and localized (with extension of order  $\sqrt{S}$ ) phase-space distributions [51]. Algebraically, the density matrix of semiclassical states is decomposed only on low rank tensors with  $K \lesssim \sqrt{S}$  in equation (2.8). The typical semiclassical states are the spin coherent states (2.4).

The operator (3.10) in the semiclassical limit tends to  $\hat{\Gamma}(\theta, \mathcal{L}^2) = 1 + O(\varepsilon^2)$ , and the evolution equation (3.13) takes the form of the classical equation of motion corresponding to the Hamiltonian (3.8); viz,

$$\partial_t W_\rho(\Omega|t) \simeq -\frac{\chi}{\varepsilon} \cos \theta \partial_\phi W_\rho(\Omega|t) = 2\varepsilon \{W_\rho(\Omega), W_H(\Omega)\}, \quad (3.17)$$

where the symbol of the Hamiltonian is

$$W_H(\Omega) \simeq \frac{\chi}{4\varepsilon^2} \cos^2 \theta. \quad (3.18)$$

The solution is defined by the classical trajectories according to equation (3.4). Nevertheless, in this case different points of the initial distribution evolve with different velocities, so that the classical motion leads to a semiclassical deformation of the initial distribution,

$$W_\rho(\Omega|t) \simeq W_\rho\left(\theta, \phi - \frac{\chi t}{\varepsilon} \cos \theta \Big|_{t=0}\right) = W_\rho(\Omega(-t)|0). \quad (3.19)$$

The evolution distorts the initial distribution but cannot convert positive regions of the Wigner function into negative regions (and vice versa) as follows from the conservation of local Poincaré invariants under the action of Poisson bracket.

Such a deformation represents, for instance, squeezing and is generated by the semiclassical current

$$J_\theta^{\text{sc}}(\Omega) = 0, \quad (3.20)$$

$$J_\phi^{\text{sc}}(\Omega) = \frac{1}{2} \frac{\chi}{\varepsilon} \sin(2\theta) W_\rho(\Omega(-t)|0).$$



In the lower panel of figure 1 we plot this semiclassical current at the same times as for the quantum case. At the initial times, both semiclassical and quantum currents look quite similar. However, already for short times,  $\tau = 0.32$ , the semiclassical distribution differs from the quantum one. The semiclassical current only produces a deformation of the initial distribution, as it follows from the (3.19). The semiclassically-evolved distribution is slightly narrower than the quantum one, but still describes very well the effect of spin squeezing [13]. For longer times, the semiclassical current keeps twisting the Wigner distribution, which obviously does not show any sort of interference pattern. The stagnation lines in the semiclassical case coincide with zeros of the evolved Wigner function, as it follows from (3.20) and differ from the quantum case, even at the initial times. Such a difference is significant and can be in principle used for a detection of genuine quantum features.

The higher moments of the Wigner distribution

$$m_k(t) = \left( \frac{2S+1}{4\pi} \right)^k \int_{\mathcal{S}_2} d\Omega W_\rho^k(\Omega|t). \quad (3.21)$$

Since in the semiclassical approximation the evolution is generated by canonical transformations, these higher moments are time-independent. The deviations from their initial values describe a spread of the initial distribution due to purely quantum effects. Actually, since  $\partial_t m(t)|_{t=0} = 0$ , the widths of the  $m_k(t)$  at  $t = 0$ , given by  $\partial_t^2 m(t)|_{t=0}$  define the timescales over which the semiclassical approximation gives a *bona fide* description of the dynamics.

#### 4. Concluding remarks

In summary, we have studied the dynamics of the Wigner function for spinlike systems and the associated phase-space flow. For linear Hamiltonians, the quantum and classical flows coincide. For nonlinear evolution, there are significant differences between quantum and classical flows, even for short times  $\tau \sim S^{-1/2}$ . From an experimental viewpoint, quantum effects can hardly be observed by measuring low-order moments of spin operators [51] when  $S \gg 1$ . Thus, by analyzing the Wigner current, in principle, it is possible to detect genuine quantum features of large spin systems arising in the course of nonlinear dynamics.

#### Acknowledgments

This work is partially supported by the Grant 254127 of CONACyT (Mexico). S. T. W. is supported by the Ministry of Science and Technology Taiwan (Grant MOST 107-2112-M-194-002). L. L. S. S. acknowledges the support of the Spanish MINECO (Grant FIS2015-67963-P).

- [1] Arnold V I 1989 *Mathematical Methods of Classical Mechanics* (Berlin: Springer)
- [2] Berry M V 1978 Regular and irregular motion *Topics in Nonlinear Dynamics (AIP Conf. Proc. vol 46)* ed Jorna S p 16
- [3] Stratonovich R L 1956 *JETP* **31** 1012—1020
- [4] Berezin F A 1975 *Commun. Math. Phys.* **40** 153–174
- [5] Hillery M, O’Connell R F, Scully M O and Wigner E P 1984 *Phys. Rep.* **106** 121–167
- [6] Lee H W 1995 *Phys. Rep.* **259** 147–211
- [7] Schroek F E 1996 *Quantum Mechanics on Phase Space* (Dordrecht: Kluwer)
- [8] Schleich W P 2001 *Quantum Optics in Phase Space* (Berlin: Wiley-VCH)
- [9] Zachos C K, Fairlie D B and Curtright T L (eds) 2005 *Quantum mechanics in phase space* (Singapore: World Scientific)
- [10] Moyal J E 1949 *Proc. Camb. Phil. Soc.* **45** 99–124
- [11] Klimov A B, Romero J L and de Guise H 2017 *J. Phys. A: Math. Theor.* **50** 323001
- [12] Ozorio de Almeida A M 1998 *Phys. Rep.* **295** 265–342
- [13] Klimov A B 2002 *J. Math. Phys.* **43** 2202–2213
- [14] Dittrich T, Gómez E A and Pachón L A 2010 *J. Chem. Phys.* **132** 214102
- [15] Polkovnikov A 2010 *Ann. Phys.* **325** 1790–1852
- [16] Bauke H and Itzhak N R 2011 *arXiv:1101.2683v1*
- [17] Steuernagel O, Kakofengitis D and Ritter G 2013 *Phys. Rev. Lett.* **110** 030401
- [18] Kakofengitis D, Oliva M and Steuernagel O 2017 *Phys. Rev. A* **95** 022127
- [19] Oliva M, Kakofengitis D and Steuernagel O 2018 *Physica A* **502** 201–210
- [20] Donoso A and Martens C C 2001 *Phys. Rev. Lett.* **87** 223202
- [21] Hughes K H, Parry S M, Parlant G and Burghardt I 2007 *J. Phys. Chem. A* **111** 10269–10283
- [22] Kakofengitis D and Steuernagel O 2017 *Eur. Phys. J. Plus* **132**
- [23] Friedman O D and Blencowe M P 2017 *arXiv:1703.04844*
- [24] Skodje R T, Rohrs H W and VanBuskirk J 1989 *Phys. Rev. A* **40** 2894–2916
- [25] Veronez M and de Aguiar M A M 2013 *J. Phys. A: Math. Theor.* **46** 485304
- [26] Veronez M and de Aguiar M A M 2016 *J. Phys. A: Math. Theor.* **49** 065301
- [27] Chaturvedi S, Marmo G and Mukunda N 2006 *Rev. Math. Phys.* **18** 887–912
- [28] Agarwal G S 1981 *Phys. Rev. A* **24** 2889–2896
- [29] Brif C and Mann A 1998 *J. Phys. A* **31** L9–L17
- [30] Heiss S and Weigert S 2000 *Phys. Rev. A* **63** 012105
- [31] Klimov A B and Chumakov S M 2000 *J. Opt. Soc. Am. A* **17** 2315–2318
- [32] Klimov A B and Romero J L 2008 *J. Phys. A* **41** 055303
- [33] Dowling J P, Agarwal G S and Schleich W P 1994 *Phys. Rev. A* **49** 4101–4109
- [34] Atakishiyev N M, Chumakov S M and Wolf K B 1998 *J. Math. Phys.* **39** 6247–6261
- [35] Chumakov S M, Frank A and Wolf K B 1999 *Phys. Rev. A* **60** 1817–1822
- [36] Chumakov S M, Klimov A B and Wolf K B 2000 *Phys. Rev. A* **61** 034101
- [37] Perelomov A 1986 *Generalized Coherent States and their Applications* (Berlin: Springer)
- [38] Varilly J C and Gracia-Bondía J M 1989 *Ann. Phys.* **190** 107–148
- [39] Fano U and Racah G 1959 *Irreducible Tensorial Sets* (New York: Academic Press)
- [40] Blum K 1981 *Density Matrix Theory and Applications* (New York: Plenum)
- [41] Varshalovich D A, Moskalev A N and Khersonskii V K 1988 *Quantum Theory of Angular Momentum* (Singapore: World Scientific)
- [42] Müller C R, Stoklasa B, Peuntinger C, Gabriel C, Řeháček J, Hradil Z, Klimov A B, Leuchs G, Marquardt C and Sánchez-Soto L L 2012 *New J. Phys.* **14** 085002
- [43] Müller C R, Madsen L S, Klimov A B, Sánchez-Soto L L, Leuchs G, Marquardt C and Andersen U L 2016 *Phys. Rev. A* **93** 033816
- [44] Tilma T, Everitt M J, Samson J H, Munro W J and Nemoto K 2016 *Phys. Rev. Lett.* **117** 180401
- [45] Bayen F, Flato M, Fronsdal C, Lichnerowicz A and Sternheimer D 1978 *Ann. Phys.* **111** 61–110
- [46] Kitagawa M and Ueda M 1993 *Phys. Rev. A* **47** 5138–5143
- [47] Agarwal G S, Puri R R and Singh R P 1997 *Phys. Rev. A* **56** 2249–2254
- [48] Corney J F, Heersink J, Dong R, Josse V, Drummond P D, Leuchs G and Andersen U L 2008 *Phys. Rev. A* **78** 023831
- [49] Rigas I, Klimov A B, Sánchez-Soto L L and Leuchs G 2013 *New J. Phys.* **15** 043038
- [50] Oliva M and Steuernagel O 2018 *arXiv:1811.02952*
- [51] Valtierra I F, Romero J L and Klimov A B 2017 *Ann. Phys.* **383** 620–634